High conductivity micro-wires in diamond following arbitrary paths

Bangshan Sun,[1] Patrick S. Salter,[1] and Martin J. Booth[1,2,a)]
[1]Department of Engineering Science, University of Oxford, Parks Road, Oxford OX1 3PJ, United Kingdom
[2]Centre for Neural Circuits and Behaviour, University of Oxford, Mansfield Road, Oxford OX1 3SR, United Kingdom

(Received 9 October 2014; accepted 18 November 2014; published online 8 December 2014)

High quality graphitic wires embedded beneath the surface of single crystal diamond are fabricated using a combination of adaptive ultrashort pulsed laser fabrication, high numerical aperture focusing, and an axial multi-fabrication scheme. Wires are created with micrometer and sub-micrometer dimensions that can follow any three dimensional path within the diamond. The measured conductivities are over an order of magnitude greater than previously reported wires fabricated by ultra-short pulsed lasers. The increased level of graphitization control in this scheme appears particularly important for fabrication of wires parallel to the diamond surface. © *2014 AIP Publishing LLC*.
[http://dx.doi.org/10.1063/1.4902998]

Diamond is truly remarkable due to the scope of exemplary material properties it possesses.[1] A promising route for the functionalization of diamond is the generation of buried electrically conductive graphitic microstructures. Such graphitic fabrication within diamond has various applications, such as all-carbon diamond radiation detectors,[2–6] metallo-dielectric photonic crystals,[7] field emitters,[8] and bolometers.[9] One method to fabricate the subsurface graphite structure is through the implantation of heavy ions, capable of fabricating ultra-thin graphite layers and three dimensional (3D) structures.[10] After an annealing process, the resistivity of the graphite was found to have a similar value to polycrystalline graphite.[10,11] The implanted graphitic structures are usually limited to a depth within $\sim 5\,\mu$m from the diamond surface. On the other hand, laser processing offers another approach to create graphitic structures in diamond. Intense ultra-short pulses create a high enough electric field magnitude at the laser focus for non-linear absorption, inducing a highly localised break down of the diamond lattice.[12] By translating the diamond through the focus, it is straightforward to trace out conductive wires. Compared to other methods, laser processing presents a much easier and quicker way to generate graphitic wires in diamond, and the fabrication can be conducted much deeper within the diamond substrate (>1.5 mm (Ref. 7)).

Since its first demonstration,[13] there have been some significant challenges to high-quality laser fabrication inside diamond. In order to generate homogeneous and uniform graphitic wires with controllable micrometre-scale dimensions, the duration of the employed laser pulse should be short enough (such as using a fs/ps pulsed laser) to minimise thermal effects.[3,6,14] However, there has previously been limited success in creating conductive wires with an ultra-short pulsed laser that have low resistivity. The current reported values are two to three orders higher than that of polycrystalline graphite.[3,6,7,15] Furthermore, it has not been possible to fabricate following an arbitrary 3D path within the diamond, with the orientation of wires restricted to the direction of the laser beam propagation, perpendicular to the diamond surface.[7,12,14–20] Recently, there have been numerous important studies investigating the properties of laser fabricated graphitic wires.[7,12,14–20] However, there is no report of ideal solution to any of these two significant challenges. The current applications of graphitic wires[2–9] are highly dependent upon their electrical properties, which suggest that a reduction of resistivity will have great impact in obtaining superior performance for the relevant devices. Additionally, whether maximising the potential of existing devices, or introducing new applications with highly complex graphite structures, the possibility to fabricate along any 3D path is extremely important. In this letter, we introduce a technique that simultaneously resolves these two existing issues through dynamic control of the laser wave-front and an axial multi-fabrication scheme.

For the fabrication, an amplified Ti:sapphire laser (SpectraPhysics Solstice) emitting 100 fs pulses with a repetition rate of 1 kHz at a wavelength of 790 nm was used as the source. Previous reports on laser processing of diamond have found a reduction in the resistivity of the graphitic wires when using a source of nanosecond pulse duration, at the expense of increased structural inhomogeneity, large irregular feature sizes, and crack formation.[3,6] Here, we are interested in generating high precision wires of ultra-thin micron/submicron dimensions and thus a femtosecond laser source is necessary. The expanded beam from the laser was directed onto a phase only liquid crystal spatial light modulator (SLM) (Hamamatsu X10468-02), which was subsequently imaged onto the pupil plane of an Olympus 1.4 NA 60× oil immersion objective lens. The sample, a single crystal CVD diamond with polished top and side surfaces, was placed on a 3D translation stage (Aerotech ABL10100 for (x–y) and ANT-95-3-V (z)) for motion control.

When focusing light into diamond, a large spherical aberration is generated due to the refractive index mismatch between the immersion medium of the objective lens ($n_L = 1.52$ for oil) and the diamond ($n_H = 2.4$).[21] In our previous research on laser fabrication in diamond, it was found that aberration correction using adaptive optical elements offered enhanced resolution[22] and enabled parallel direct

a)Electronic mail: martin.booth@eng.ox.ac.uk

writing.[23] In this letter, we aim to generate extended wires following 3D paths beneath the surface of diamond, and as such, the aberration correction needs to be adjusted real-time according to the fabrication depth. To achieve this, a single SLM is included within the experimental system to dynamically control the wavefront of the fabrication laser.

The orientation of the fabrication is explained in Figs. 1(a) and 1(b). As demonstrated by the theoretical focal energy distribution in Fig. 1(a1), the focus of the flat incident wave-front is seriously distorted, elongated, and non-uniform along the z axis. The peak two-photon intensity reduces to 17% when focusing to a depth of 20 μm. This distortion increases with fabrication depth.[21] In comparison, the dynamically adjusted incident wave front enables a highly confined laser focus at different target depths (Fig. 1(b1)). The appropriate phase for aberration compensation at a particular depth was calculated[23] and then implemented in experiment using position feedback from the sample translation stages to update the phase patterns displayed on the SLM in real-time. Comparing the sketches in Figs. 1(a1) and 1(b1), we can see that the corrected beam (b1) offers far better control over the fabrication process and wire size. The major focal distortion in (a) is along the z direction, while the focal dimensions are not as seriously affected along the x or y axis. This indicates the reason why previous laser fabrication in diamond has always been successful along the direction of beam propagation (z axis),[7,12,14–20] but very limited in all other directions. If we look at the wires parallel to the surface in an experiment, the structural modifications for the uncorrected beam in (a2) are much larger and crucially give rise to high non-uniformity in the conversion from diamond to graphite. There appear to be regions inside the laser processed area along the irradiated path where the diamond is unaffected by the laser. In contrast, the structural modification arising from an undistorted focus (b2) shows good confinement along the z axis and a high level of uniformity. There are no obvious regions where the diamond lattice remains unmodified following fabrication. Both wires have a length of 70 μm in the x direction. The resistance for the wire fabricated with the distorted focus (a2) is found to be beyond the range of our measurement apparatus (>30 MΩ, corresponding to a resistivity >1700 Ω cm). In contrast, the wire in (b2) has a measured resistance of 20 kΩ (resistivity ~0.1 Ω cm). The significant difference in the resistivity is strongly related to the degree of distortion in the laser focus. The high spatial confinement achieved when aberrations are cancelled causes the diamond lattice to be broken down only within a small focal volume. This seems to enable a higher conversion rate to the graphitic phase, thus increases the wires conductivity.

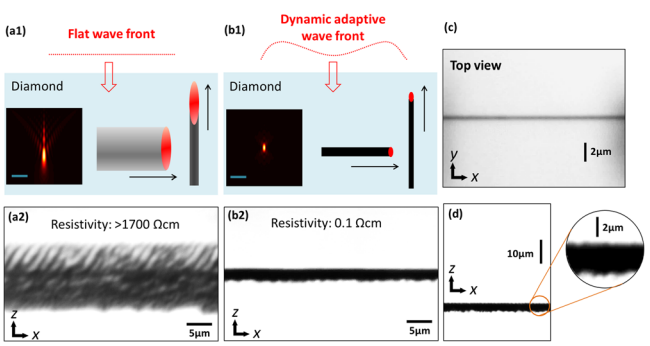

FIG. 1. Fabrication of graphitic wires using an ultrafast laser with a flat incident wave-front (a) and adaptive wave-front control (b). (a1) and (b1) Theoretical calculation of the focal intensity distribution at a depth of 20 μm (scale bar is 2 μm) and illustration of fabrication perpendicular and parallel to the diamond surface. (a2) and (b2) Wide-field optical transmission microscope images showing associated wires fabricated parallel to the diamond surface at a depth of 20 μm. (c) An ultra-thin graphitic conductive wire with a width of 0.4 μm. (d) A conductive wire fabricated parallel to the surface with aberration compensation at a depth of 100 μm in diamond. The fabrication laser beam was incident along the negative z direction.

The dimensions of the fabricated wire can be reduced by fine control over the laser power. An ultra-thin wire with a width 400 nm was fabricated with a power of 6 μW (pulse energy of 6 nJ), making it the smallest reported laser-induced graphitic wire inside diamond. An image of such a wire is shown in Fig. 1(c). We note that the size was approaching the resolution limit of the optical transmission microscope used for inspection, and thus 400 nm places an upper limit on the actual size. Furthermore, the resistivity of this ultra-thin wire was measured as <0.4 Ω cm. This is already an improvement over other reported wires written with ultra-short lasers – even those wires of much larger cross-section size, whose reported resistivity varied from 0.9 to 3.9 Ω cm.[3,6,7,15]

Fig. 1(d) shows a wire fabricated parallel to the surface at a depth of 100 μm in the diamond. The wires were similar in morphology and were fabricated at comparable pulse energy as those at shallower depths confirming successful correction of the aberration. The resistivity of the wires fabricated at different depths within the diamond was found to be similar, indicating that the nature of material modification in this fabrication scheme did not depend upon the fabrication depth.

A detailed study of the electrical properties for the subsurface wires was conducted with different parameters. In order to measure the resistance of the wires inside the diamond, two graphitic pillars with a cross-section size of ~5 × 5 μm were fabricated to connect the wire to the surface, which is shown in Fig. 2(a). Surface contacts with a size of ~12 × 12 μm were also fabricated subsequently using a dry objective lens (Zeiss 0.5 NA). A micro-positioner rig with probe tips (diameter 10 μm) was used to make electrical contact with the embedded graphitic wires. The resistance was measured by an Agilent 4192A LF impedance analyzer. The resistance was found to be >30 MΩ if one probe touched the graphite surface contact when the other probe touched the native diamond surface; the resistance was 0.5 Ω if the two probes touched the surface of a gold contact separated by a distance of 100 μm.

Here, we introduce an axial multi-fabrication scheme, which is able to reduce the resistivity and precisely control the wire size. As illustrated in Fig. 2(a), the whole wire is fabricated by several passes of the diamond through the laser focus with a slight axial shift in the focal position between each pass. Example wires shown in Figs. 2(b) and 2(c) were fabricated with four passes with axial shift of 0.5 μm, parallel to the diamond surface at a depth of 20 μm, speed of 10 μm/s with a laser power of 20 μW (pulse energy of 20 nJ). The approximately elliptical cross-section of such a wire was

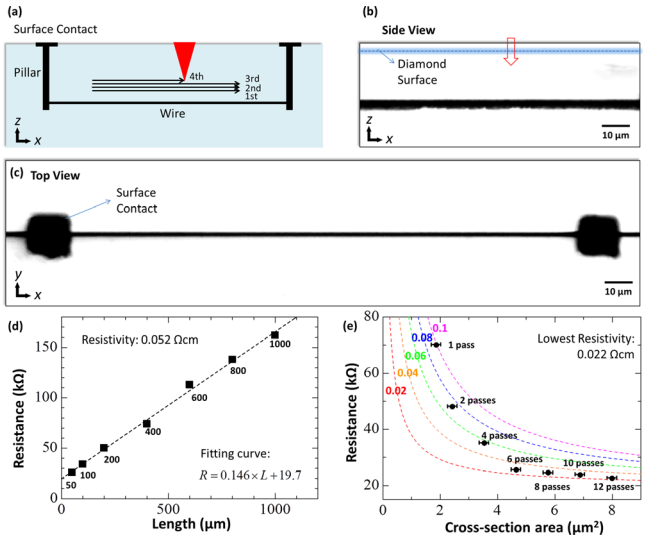

FIG. 2. (a) Sketch of axial multi-fabrication scheme, and the structure of embedded wire contacts and pillars. (b) Side view and (c) top view optical microscope images of the wire for resistance measurement. (d) Resistance as a function of the wire length parallel to the surface. (e) Resistance as a function of the wire cross-sectional area. The dashed colored curves show the theoretical prediction for wires with different resistivities (marked on the left, in units of Ω cm).

measured to have minor and major axes of 1.4 μm and 3.2 μm ($\pm\sim$5%), respectively. We note that the lower edge of the fabricated wire in Fig. 2(b) appears less uniform compared to the other edges. We believe that this may be due to graphite generation arising from the first incident pulses absorbing the energy of subsequent pulses, which results in reduced illumination at the lower edge, removing the possibility for a cumulative fabrication effect that can smooth out the material modification.

A set of wires were fabricated, each with equal cross-section but different lengths ranging from 50 μm to 1000 μm. The resistance of each wire was measured and is shown in Fig. 2(d). There is a linear increase in resistance R with wire length L as would be expected from the relationship: $R = L\rho/S$, where ρ is the resistivity and S is the cross-sectional area. This allows us to obtain the average resistivity of 0.052 Ω cm (±5%) from the gradient of the linear fit. It is seen that there exists an additional resistance of 19.7 kΩ when the wire length is extrapolated to zero, arising from the resistance of the pillar and surface contact, as well as any additional contact losses between the measuring probe tips and surface contacts. The pillars and surface contacts for each of the wires were fabricated in sequence under identical conditions. Therefore, this additional loss is considered to be a fixed constant for all the wires.

Wires of varying cross-section were generated using the axial multi-fabrication scheme by changing the number of spatially shifted passes. The measured resistance is shown in Fig. 2(e) as marked points. As a guide, several theoretically calculated curves, taking into account the additional contact losses of 19.7 kΩ, are also shown. The resistivity reduction effect of the axial multi-fabrication scheme is clearly seen. The resistivity was reduced from 0.1 Ω cm to 0.022 Ω cm by increasing the number of passes from 1 to 12. As discussed above, the lower edge of the graphitic wire generally appears rougher than the upper section. Therefore, by gradually increasing the number of additional laser passes above the initial wire along the z direction, the proportion of well-formed graphite increased, resulting in a reduction of resistivity for the whole wire. The effect of increasing the number of passes on the resistivity is more pronounced for a low number of passes (up to 6), and then the resistivity value becomes relatively stable (from 6 to 12 passes). This minimum resistivity we obtained here (0.022 Ω cm, corresponding to a conductivity of 4545 S/m) was reduced by a factor of 40 to 180 times compared to the previously reported resistivities of fs/ps induced wires: 1.6 Ω cm,[7] 3.9 Ω cm,[15] and 0.9 Ω cm.[3,6] We therefore conclude that this was the lowest resistivity ever achieved for a laser written graphitic wire inside diamond.

We note that both the cross-section size and resistivity of the generated wires are related to the incident laser power. Lower powers reduce the cross-section dimensions, whilst also resulting in higher resistivity. Interestingly, we further observe that increasing the laser power does not lead to an endless reduction in the resistivity. Rather, for powers above an optimum value, the resistivity presents a rising trend. Laser pulse energies of 30 nJ and 60 nJ were used to fabricate the wires with a single pass. The measured resistivity was 0.19 Ω cm and 0.37 Ω cm, respectively. These values were higher than the 0.1 Ω cm resistivity for wires created by pulse energy of 20 nJ discussed above. For pulse energies above the optimum, the fabrication process generates larger regions of poor quality conductor around the laser focus, thus reducing the whole quality of the wire.

When using an ion implantation graphitisation method, it was found that a high temperature anneal process could reduce the resistivity of the wires by several orders of magnitude.[10] However, our preliminary experimental results following an anneal process where the diamond was maintained at 1100 °C for 1 h in a vacuum of at least 10^{-5} mbar did not show a noticeable reduction in resistivity for the laser induced graphitic wires. This may be related to the different underlying mechanisms behind graphitization in ion implantation and laser fabrication but is subject to further investigation.

Until now, laser fabrication has been very limitedly reported on the 2D/3D graphitic wires in diamond. A unique advantage of this fabrication scheme is the ability to fabricate with high precision along any direction, which enables the creation of highly conductive single 2D/3D wires with arbitrary shape. To demonstrate this ability, we show two representative shapes: a spiral and a helix. Fig. 3(a) shows an image of the spiral wire, prior to the fabrication of the vertical conductive pillars. The spiral wire has an inner radius that increases from 10 μm to 24 μm. After fabricating pillars and surface contacts, the resistivity was measured to be 0.05 Ω cm (±5%), which is close to that of the straight four-pass wires in Fig. 2 (0.052 Ω cm). Top view and side view images of a helical wire are shown in Figs. 3(b) and 3(c). The helix dimensions along the x, y, and z directions are 40 μm, 20 μm, and 20 μm, respectively. A SHG (second harmonic generation[24]) microscope is used to image the structure with 3D resolution in Fig. 3(d). It is worth noting that the fabrication additionally causes stress in the surrounding diamond, due to

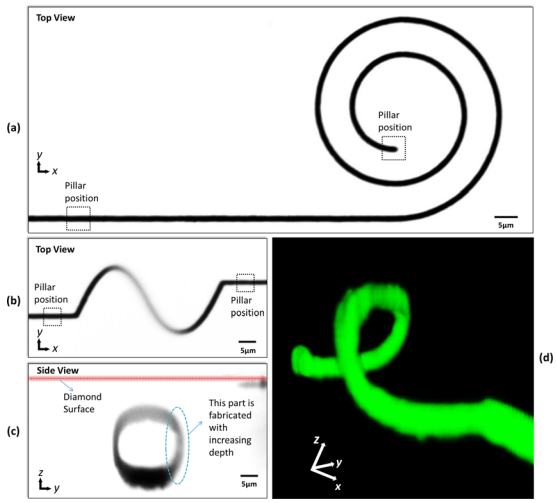

FIG. 3. Examples of single wires following spiral and helical paths. Both wires were fabricated with four axially shifted passes of the laser beam. The depth of the helical wire ranged from 10 to 30 μm. The positions of subsequent pillar fabrication are marked in the images. (a) Optical transmission microscope image of the spiral wire. (b) Top view and (c) side view of helical wire. (d) 3D SHG microscope image of the helical wire.

the lower density of the generated graphitic phase, and the stressed region is also detected in the SHG microscope. Thus, the wire cross-section in the SHG image appears larger and the surface rougher than in the transmission microscope image. Further investigations are being undertaken to ascertain the effect of the generated stress field on the surrounding properties of the diamond. The measured resistivity of the helical wire was 0.13 Ω cm (±5%). Compared to the straight wires, one potential cause for the slight rise in resistivity is that part of the wire (marked in Fig. 3(c)) was fabricated by translating the focus downward through the diamond, such that previous material modification partially obscured the incident beam from the updated focal position. This problem could be circumvented by adopting a straightforward bottom up fabrication strategy.

In summary, we have demonstrated several significant advances for the generation of graphitic wires in diamond, including wires that are not only highly conductive but also able to follow any 3D path; the lowest reported resistivity of 0.022 Ω cm, approaching that of polycrystalline graphite; and the smallest laser written conductive nano-wire with a width of <400 nm and resistivity of <0.4 Ω cm. This could not only benefit the wide range of emergent applications that combine diamonds properties with electrical measurement and control, from quantum enhanced technologies,[25] semiconductor research,[26] to sensor based devices either for the detection of ionizing radiation[3,6] or for use in harsh environments,[27] but also offer the opportunity for the versatile design of high quality, more complex 3D graphitic structures in diamond.

We greatly thank Dr. Crisanto Quintana Sanchez and Mr. Grahame Faulkner in providing the micropositioner rigs for the measurement of resistance in the graphitic wires. We also acknowledge useful discussions with Dr. Brian Patton and Dr. Jason Smith and thank Mr. Xiang Liu in assisting with the SHG microscopy. This research was funded by the Leverhulme Trust (Grant No. RPG-2013-044).

[1]I. Aharonovich, A. D. Greentree, and S. Prawer, Nat. Photonics **5**, 397 (2011).
[2]A. Oh, B. Caylar, M. Pomorski, and T. Wengler, Diamond Relat. Mater. **38**, 9 (2013).
[3]S. Lagomarsino, M. Bellini, C. Corsi, F. Gorelli, G. Parrini, M. Santoro, and S. Sciortino, Appl. Phys. Lett. **103**, 233507 (2013).
[4]B. Caylar, M. Pomorski, and P. Bergonzo, Appl. Phys. Lett. **103**, 043504 (2013).
[5]T. Kononenko, V. Ralchenko, A. Bolshakov, V. Konov, P. Allegrini, M. Pacilli, G. Conte, and E. Spiriti, Appl. Phys. A: Mater. Sci. Process. **114**, 297 (2014).
[6]S. Lagomarsino, M. Bellini, C. Corsi, S. Fanetti, F. Gorelli, I. Liontos, G. Parrini, M. Santoro, and S. Sciortino, Diamond Relat. Mater. **43**, 23 (2014).
[7]M. Shimizu, Y. Shimotsuma, M. Sakakura, T. Yuasa, H. Homma, Y. Minowa, K. Tanaka, K. Miura, and K. Hirao, Opt. Express **17**, 46 (2009).
[8]A. V. Karabutov, V. G. Ralchenko, I. I. Vlasov, R. A. Khmelnitsky, M. A. Negodaev, V. P. Varnin, and I. G. Teremetskaya, Diamond Relat. Mater. **10**, 2178 (2001).
[9]T. I. Galkina, A. Y. Klokov, A. I. Sharkov, R. A. Khmelnitski, A. A. Gippius, V. A. Dravin, V. G. Ralchenko, and A. V. Savelev, Phys. Solid State **49**, 654 (2007).
[10]F. Picollo, D. Gatto Monticone, P. Olivero, B. A. Fairchild, S. Rubanov, S. Prawer, and E. Vittone, New J. Phys. **14**, 053011 (2012).
[11]A. Reznik, V. Richter, and R. Kalish, Phys. Rev. B **56**, 7930 (1997).
[12]V. I. Konov, Laser Photonics Rev. **6**, 739 (2012).
[13]S. Prawer and D. N. Jamieson, Phys. Rev. Lett. **69**, 2991 (1992).
[14]T. V. Kononenko, M. S. Komlenok, V. P. Pashinin, S. M. Pimenov, V. I. Konov, M. Neff, V. Romano, and W. Lüthy, Diamond Relat. Mater. **18**, 196 (2009).
[15]T. V. Kononenko, V. I. Konov, S. M. Pimenov, N. M. Rossukanyi, A. I. Rukovishnikov, and V. Romano, Diamond Relat. Mater. **20**, 264 (2011).
[16]V. N. Strekalov, V. I. Konov, V. V. Kononenko, and S. M. Pimenov, Appl. Phys. A: Mater. Sci. Process. **76**, 603 (2003).
[17]T. V. Kononenko, M. Meier, M. S. Komlenok, S. M. Pimenov, V. Romano, V. P. Pashinin, and V. I. Konov, Appl. Phys. A: Mater. Sci. Process. **90**, 645 (2008).
[18]M. Neff, T. V. Kononenko, S. M. Pimenov, V. Romano, W. Lüthy, and V. I. Konov, Appl. Phys. A: Mater. Sci. Process. **97**, 543 (2009).
[19]S. M. Pimenov, I. I. Vlasov, A. A. Khomich, B. Neuenschwander, M. Muralt, and V. Romano, Appl. Phys. A: Mater. Sci. Process. **105**, 673 (2011).
[20]T. V. Kononenko, A. A. Khomich, and V. I. Konov, Diamond Relat. Mater. **37**, 50 (2013).
[21]B. Sun, P. S. Salter, and M. J. Booth, J. Opt. Soc. Am. A **31**, 765 (2014).
[22]R. D. Simmonds, P. S. Salter, A. Jesacher, and M. J. Booth, Opt. Express **19**, 24122 (2011).
[23]A. Jesacher and M. J. Booth, Opt. Express **18**, 21090 (2010).
[24]G. D. Marshall, A. Jesacher, A. Thayil, M. J. Withford, and M. Booth, Opt. Lett. **36**, 695 (2011).
[25]F. Jelezko and J. Wrachtrup, Phys. Status Solidi A **203**, 3207 (2006).
[26]S. A. O. Russell, S. Sharabi, A. Tallaire, and D. A. J. Moran, IEEE Electron Device Lett. **33**, 1471 (2012).
[27]S. D. Janssens, S. Drijkoningen, and K. Haenen, Appl. Phys. Lett. **104**, 073107 (2014).